Table 19.1 Moments and disposition parameters of ^{32}P-pDNA and ^{32}P-oligonucleotides in the single-pass rat liver perfusion system

		Moment parameters		*Disposition parameters*				
Compound	*Dose* (μg/liver)	*AUC* (% dose sec/mL)	*t(bar)* (sec)	*V* (mL/g tissue)	t_{cor} (min)	*E (%)*	k_{el} (min^{-1})	CL_{int} (mL/min/g tissue)
^{32}P-pDNA[a]	1.33	252 ± 17	12.6 ± 1.5	0.598 ± 0.09	0.313 ± 0.05	45.6 ± 0.3	21.7 ± 0.1	1.29 ± 0.12
	13.3	365 ± 14	10.3 ± 1.0	0.314 ± 0.08	0.179 ± 0.03	20.1 ± 0.8	1.17 ± 0.09	0.354 ± 0.10
^{32}P-PO[b]	3	402 ± 19	16.6 ± 1.5	0.691 ± 0.09	0.333 ± 0.02	15.3 ± 1.8	0.434 ± 0.17	0.214 ± 0.08
^{32}P-PS_3[b]	0.3	264 ± 27	20.8 ± 2.0	0.796 ± 0.02	0.408 ± 0.03	45.4 ± 8.5	1.45 ± 0.19	1.15 ± 0.85
	3	320 ± 12	17.2 ± 8.8	0.746 ± 0.40	0.314 ± 0.03	33.2 ± 3.1	0.857 ± 0.56	0.786 ± 0.61
	30	446 ± 6	12.5 ± 0.7	0.315 ± 0.01	0.214 ± 0.01	3.00 ± 0.84	0.162 ± 0.10	0.051 ± 0.03
^{32}P-PS[b]	3	289 ± 5	41.7 ± 2.4	1.55 ± 0.14	1.08 ± 0.09	35.8 ± 0.9	0.516 ± 0.04	0.798 ± 0.01
^{51}Cr-RBC[c]	–	471	8.89	0.209	0.148	0	–	0
^{131}I-HSA[C]	–	486	9.33	0.252	0.156	0	–	0

Notes
PO, PS_3, PS, 20-mer antisense oligonucleotide complementary to the human c-*myc* mRNA with different internucleotide linkages; PO, phosphodiester; PS_3, three phosphorothioate linkages on both ends; PS, phosphorothioate. RBC, red blood cells; HSA, human serum albumin. a Yoshida *et al.*, 1996; b Takakura *et al.*, 1996; c Nishida *et al.*, 1989.

interact with the tissue, its V value is close to the volume of the blood vessels within the liver. Compared with ^{131}I-human serum albumin (HSA), a vascular reference substrate that distributes the sinusoidal and Disse spaces in the liver, all gene drugs listed in Table 19.1 had larger V value, indicating their reversible interaction with the tissue. During the 60 minute perfusion, radioactivity could be detected in the outflow when ^{32}P-PS was bolusly administered into the liver (Takakura *et al.*, 1996), showing a very slow dissociation of the ^{32}P-PS oligonucleotide attached onto the surface of liver cells. The reversible (V) and irreversible (E) parameters of these gene drugs decreased with an increasing dose, indicating that both interactions are saturable processes.

Constant infusion

Contrary to the bolus input experiment that is particularly useful for examining the initial stages of hepatic uptake of drugs, constant infusion gives direct information on the uptake behavior of drugs at steady state. In particular, slow processes can be clearly characterized by this approach. Furthermore, the binding and internalization processes can be distinguished from each other (Nishida *et al.*, 1992). When a drug is constantly supplied to the liver, a fraction would be steadily extracted by the tissue, and the extraction ratio at steady state (E_{ss}) for the drug is calculated as follows:

$$E_{ss} = \frac{C_{in,ss} - C_{out,ss}}{C_{in,ss}} \tag{17}$$

where $C_{in,ss}$ and $C_{out,ss}$ are the concentration of the drug in the perfusate before and after passing through the liver under steady state condition. Then (at steady state), the hepatic clearance (CL_h, mL/min) of the drug is expressed as:

$$CL_h = E_{ss} \cdot Q \tag{18}$$

where Q (mL/min) is the perfusion rate.

To obtain the binding and internalization parameters of a drug, a physiological one-organ model is employed as shown in Figure 19.5 (Nishida *et al.*, 1992). In this model, the sinusoidal compartment, consisting of the vascular and Disse spaces, is assumed to be under, a well stirred condition, and the concentration is assumed to be similar to that in the outflow (C_s, corresponding to $C_{out,ss}$ in Eq 17; C_b equals to $C_{in,ss}$). The binding compartment is characterized by a maximum binding amount (X_∞) and a binding constant (K) and rapid equilibration is assumed to occur between the sinusoidal and binding compartments. V_s represents the sum of the volumes of the sinusoid and Disse spaces (assumed to be 0.180 mL/g liver). Assuming the internalization process follows a first-order rate kinetics, the internalization rate of a drug (dX/dt) is expressed as a product of a binding amount X and its rate constant (k_{int}). Then, in the sinusoidal and binding compartments, a mass-balance equation is defined as follows:

$$V_s\left(\frac{dC_s}{dt}\right) + \left(\frac{dX}{dt}\right) = QC_b - QC_s - k_{int}X \tag{19}$$

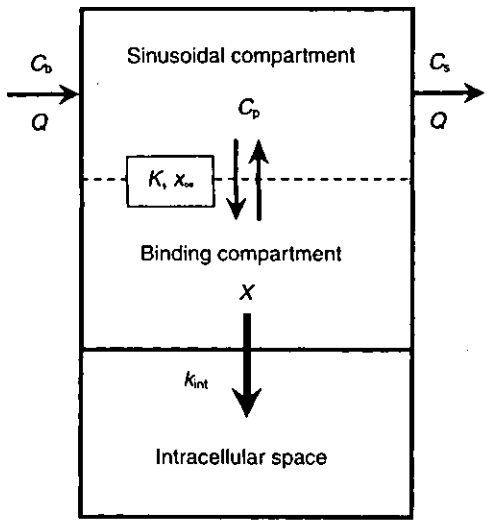

Figure 19.5 Physiological pharmacokinetic model for hepatic uptake of drug constantly infused in the isolated rat liver perfusion system. Q, flow rate (mL/min); C_b, inflow concentration (μg/mL); C_s, sinusoidal concentration (μg/mL); V_s, sinusoidal volume (mL); X, binding constant (μg); X_∞, maximum binding amount (μg); K, binding constant (mL/μg); k_{int}, internalization rate constant (min^{-1}).

Assuming the binding of a drug to the cell surface is consistent with the Langmuir equation, the following expression holds:

$$X = \frac{X_\infty K C_s}{1 + K C_s} \tag{20}$$

Differentiated with respect to t (time), Eq 20 is changed to

$$\frac{dX}{dt} = \frac{X_\infty K}{(1 + K C_s)^2}\left(\frac{dC_s}{dt}\right) \tag{21}$$

To substitute Eq (19) with Eq (21) gives the following equation:

$$\left(V_s + \frac{X_\infty K}{(1 + K C_s)^2}\right)\left(\frac{dC_s}{dt}\right) = QC_b - QC_s - \left(\frac{k_{int} X_\infty K C_s}{1 + K C_s}\right) \tag{22}$$

When the constant infusion experiments are performed at various inflow concentrations of a drug, the differential equations are numerically solved (Nishida *et al.*, 1992; Ogawara *et al.*, 1998, 1999).

When ^{32}P-pDNA was constantly infused in the isolated perfused rat liver, however, its uptake by the perfused liver did not reach a steady state during the experimental period of 60 minutes (Yoshida *et al.*, 1996). Therefore, a precise analysis of the binding and internalization characteristics could not be performed.

Isolated perfused kidney

The same statistical analytical method used for the liver can be applied to examine the disposition characteristics of a drug in the kidney. The following parameters are important to understand the renal disposition of drug:

$$AUC = \int_0^\infty C dt \tag{23}$$

$$MTT_{kid} = \int_0^\infty \frac{tC}{AUC} dt \tag{24}$$

$$F_u = \int_0^\infty \left(\frac{dX_u}{dt}\right) dt \tag{25}$$

$$MTT_u = \frac{\int_0^\infty t\left(\frac{dX_u}{dt}\right) dt}{F_u} \tag{26}$$

where MTT_{kid} (sec) is the mean transit time of drug in the kidney; F_u denotes the urinary recovery (excretion) ratio; dX_u/dt is the urinary excretion rate, and MTT_u is the urinary mean excretion time. Then the distribution volume at steady state (V_d) is calculated from these moment parameters as follows:

$$F_0 = AUC \cdot Q \tag{27}$$

$$V_d = \frac{Q \cdot MTT_{kid}}{F_0} \tag{28}$$

where F_0 is the venous outflow recovery ratio. By adjusting the renal arterial pressure (from 70–80 to 55 mmHg) and tying off the ureters, one can have a 'nonfiltering' kidney, in which the glomerular filtration does not occur. This technique is useful to distinguish events occurring in the capillary side of the kidney from those in the luminal side.

Reference substances are required to understand the pharmacokinetic characteristics of a gene drug in the perfused kidney. Serum albumin can be used as a marker that is hardly filtered at the kidney and rarely taken up by the tissue through the passage. Inulin is a well-known marker of glomerular filtration rate. These references have unique pharmacokinetic parameters when subjected to the pharmacokinetic analysis in the isolated perfused rat kidney (Table 19.2). Oligonucleotides with different internucleotide linkages are found to have significant reversible interaction with the kidney (because they have larger MTT_{kid} and V_d, parameters representing reversible interaction, than those reference substances) (Sawai *et al.*, 1995, 1996).

Tissue-isolated perfused tumor

The pharmacokinetics of a gene drug within tumor tissue is a very important issue because cancer becomes one of the major targets for gene therapy, and various protocols are now under clinical trials (Roth and Cristiano, 1997). For *in vivo* gene delivery protocols, a gene drug, free or complexed with vector, is sometimes

Table 19.2 Moments and distribution volume of ^{32}P-pDNA and ^{32}P-oligonucleotides in the single-pass rat kidney perfusion system

Compound	*Dose* (μg/kidney)	*AUC* (% dose sec/mL)	MTT_{kid} (sec)	V_d (mL)
^{32}P-PO[a]	0.42	376 ± 4	1.45 ± 0.07	0.462 ± 0.013
^{32}P-PS$_3$[a]	0.42	335 ± 1	1.51 ± 0.12	0.491 ± 0.011
^{32}P-PS[a]	0.42	319 ± 23	2.54 ± 0.14	0.716 ± 0.022
^{14}C-Inulin[b]	–	352 ± 49	1.42 ± 0.10	0.449 ± 0.021
^{111}In-BSA[b]	–	302 ± 12	0.900 ± 0.014	0.240 ± 0.001

Notes
PO, PS$_3$, PS, 20-mer antisense oligonucleotide complementary to the human c-*myc* mRNA with different internucleotide linkages; PO, phosphodiester; PS$_3$, three phosphorothioate linkages on both ends; PS, phosphorothioate; BSA, bovine serum albumin. a Sawai *et al.*, 1996; b Mihara *et al.*, 1993a.

injected directly into tumor tissues (Kitajima *et al.*, 1992; Ratajczak *et al.*, 1992; Plautz *et al.*, 1993; Sun *et al.*, 1995; Wei *et al.*, 1995; Toloza *et al.*, 1996; Dow *et al.*, 1998; Nemunaitis *et al.*, 1999) because the direct administration circumvents vascular and interstitial barriers in the systemic delivery of a gene drug to the tumor. Injected intratumorally, a gene drug would distribute within the tissue, and fractions reaching to the blood vessel would be cleared by blood flow, so the profiles of the drug in the outflow include information on their disposition characteristics within the tumor tissue (Saikawa *et al.*, 1996). Quantitative evaluation of its disposition within the tumor tissues is important to assess and predict the efficiency of *in vivo* cancer gene therapy. A tissue-isolated tumor is a good experimental system to investigate the intratumoral disposition of pharmaceuticals, because (i) experimental conditions are easily controlled, (ii) its disposition features in the tumor tissue can be obtained independently from those in other normal tissues, and (iii) disposition characteristics can be quantitatively analyzed by a pharmacokinetic approach.

Since Gullino and Grantham reported in 1961 the use of a tissue-isolated tumor in studying exchanges of fluids between host and tumor, their model has been used in estimating physiological properties of tumors, such as blood flow, interstitial pressure, and energy metabolism, and in evaluating the effect of interstitial pressure on the distribution of macromolecules. In their model, blocks of Walker 256 carcinoma are inoculated in the adipose tissue around the ovary and enclosed in a plastic bag to separate it from other tissues. After an adequate period, the tumor, isolated from other tissues, can be perfused after being cannulated with tubes into the aorta and vena cava. To ensure independent perfusion for the isolated tumor, all blood vessels supplying other tissues (left renal artery and vein, right renal vein, inferior vena cava, and aorta) should be ligated. After administration of a drug, the outflowing perfusate is collected at appropriate time intervals for analysis. Figure 19.6 shows a scheme of the experimental system of the tissue-isolated tumor of Walker 256 carcinosarcoma.

Some physiological parameters of this tissue-isolated tumor vary among preparations. Necrosis can be apparently observed near the center of the tissue with the increase in the size of the tumor (Warren, 1970; Leunig *et al.*, 1992; Fox *et al.*, 1993). Therefore, the blood supply to the tissue is highly heterogeneous and, in this case, the tumor tissue can be divided into a well perfused (viable) region and

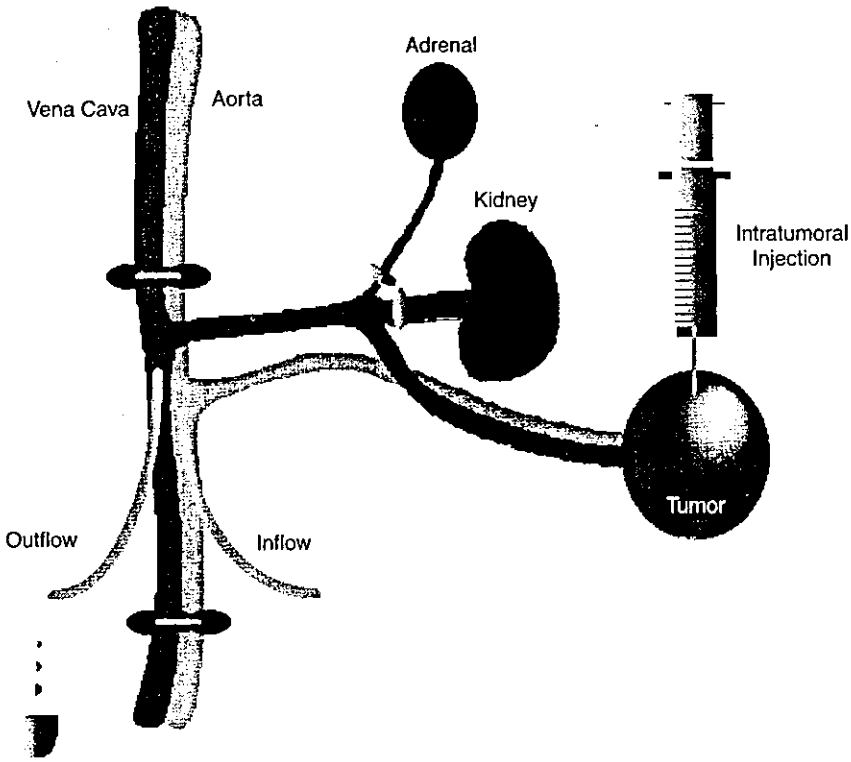

Figure 19.6 Schematic presentation of perfusion system of the tissue-isolated tumor preparation.

a poorly perfused (necrotic and/or hypoxic) region. Fluid regularly oozes out from the tumor surface (Butler *et al.*, 1975), but the fluid leakage is highly unique, for each tumor preparation and its rate hardly correlates with the size of the tumor (Saikawa *et al.*, 1996). Therefore, the tumor tissue can be divided into two regions, viable and necrotic regions. Large tumors possess widespread necrotic regions that are poorly perfused with blood. On the other hand, viable regions are enriched with vasculature. Based on these results and anatomical characteristics of tumor tissues, a pharmacokinetic model to evaluate the intratumoral behavior of a drug after intratumoral injection is developed (Figure 19.7). In the model, the tumor tissue is assumed to be composed of two compartments, well perfused and poorly perfused regions. A drug in the well perfused region is assumed to be cleared from the vascular side quickly and in the poorly perfused region it is assumed to be transferred to the well perfused region or leak out. The poorly perfused region is assumed to have little blood supply and also to contain some necrotic tissue. The well perfused region, in contrast, is assumed to consist of vascular space and its surrounding space, which is in equilibrium to the vascular space. Based on these assumptions, the following equations are derived to describe the change in the drug amount in these two regions with time:

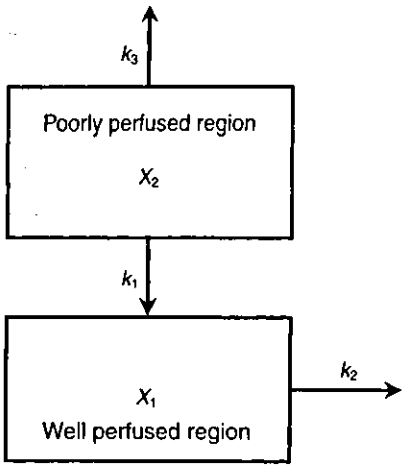

Figure 19.7 Pharmacokinetic model for analyzing drug disposition following direct intratumoral injection. k_1, rate constant of transfer from poorly perfused region to well perfused region; k_2, venous appearance rate constant; k_3, rate constant of leakage from the surface; X_1 and X_2, drug amounts in well perfused and poorly perfused regions, respectively.

$$\frac{dX_1}{dt} = k_1X_2 - k_2X_1 \tag{29}$$

$$\frac{dX_2}{dt} = -(k_1 + k_3)X_2 \tag{30}$$

where X_1 and X_2 are drug amounts in well and poorly perfused regions, respectively; k_1 is the rate constant of transfer from poorly perfused regions to well perfused regions; k_2 is the venous appearance rate constant; and k_3 is the rate constant of leakage from the surface. The integration of Eq (29) and (30) gives

$$J = Ae^{-\alpha t} + Be^{-\beta t} \tag{31}$$

$$A = k_2X_0\frac{k_1 + (1 - R)(k_3 - k_2)}{k_1 + k_3 - k_2} \tag{32}$$

$$B = -\frac{k_1k_2RX_0}{k_1 + k_3 - k_2} \tag{33}$$

$$\alpha = k_2 \tag{34}$$

$$\beta = k_1 + k_3 \tag{35}$$

where J (% of dose/min) is the appearance rate in venous outflow, which is equal to k_2X_1; X_0 is the injected dose; and R is the dosing ratio into the poorly perfused region. To estimate the pharmacokinetic parameters, k_1, k_2, k_3 and R, the venous outflow pattern is fitted to Eq (31).

This pharmacokinetic model has been applied to analyze the intratumoral disposition characteristics of lipidic drug carriers (Nomura *et al.*, 1998a), macromolecular prodrugs of MMC (Nomura *et al.*, 1998b), and naked pDNA (Nomura *et al.*, 1997). Some parameters obtained based on the model vary among tumor preparations, depending on their sizes (Saikawa *et al.*, 1996). Therefore, in order to use the pharmacokinetic model for evaluating the intratumoral behavior of a drug, the sizes of the tumor preparations should be controlled. Figure 19.8 summarizes the pharmacokinetic parameters, k_1 and k_2, representing the transfer rate within the tissue and the venous appearance rate, respectively, of ^{32}P-pDNA and other test compounds. Extensive differences in the physicochemical properties of test compounds, i.e., from low-molecular weight drugs like mitomycin C (MMC, MW 334) to particulate lipidic carriers like fat emulsions (mean diameter of 250 nm), slightly affected k_1, but greatly influenced k_2, indicating that the rate of transfer from the poorly perfused compartment to the well perfused compartment is the determining factor that controls the intratumoral behavior of a drug following its direct injection. In Figure 19.8, cationic liposome shows the smallest k_1 value, and cationic MMC-dextran conjugate (MMC-Dcat) has a larger k_1 than anionic conjugate (MMC-Dan); these results indicate that the electrical interaction of a cationic drug with the anionic surface of the tissue prolongs the drug's retention in the tumor. Furthermore, pDNA-cationic liposome complex injected in the tumor was

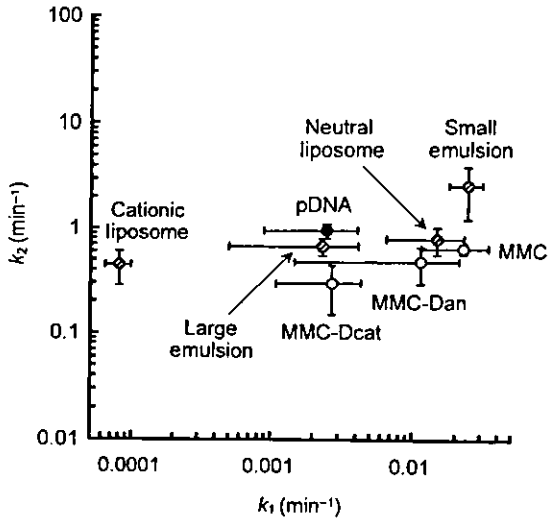

Figure 19.8 Pharmacokinetic parameters, k_1 and k_2, following direct intratumoral injection of drugs in tissue-isolated tumor. k_1 is the rate constant of transfer of drug from poorly perfused region to well perfusion region, and k_2 is the venous appearance rate constant of drug. MMC, mitomycin C; MMC-Dan, MMC conjugate with anionic dextran (T-70); MMC-Dcat, MMC conjugate with cationic dextran (T-70); Large Emulsion, egg phosphatidylcholine (PC)/soybean oil emulsion with diameter of 250 nm; Small Emulsion, egg PC/soybean oil emulsion with diameter of 86 nm; Neutral Liposome, egg PC/dioleoylphosphatidylethanolamine (DOPE) liposome with diameter of 120 nm; Cationic Liposome, Liposome, egg PC/DOPE/dimethyldioctadecylammonium liposome with diameter of 125 nm.

hardly recovered in the outflow (Nomura *et al.*, 1997). In such cases, the pharmacokinetic analysis cannot be performed because the analysis uses the venous appearance rate of drug.

CONCLUDING REMARKS

It is important to develop vector and/or transfection methods that enable us to achieve gene expression *in vivo* that is high in its efficiency and long in its duration. Understanding the elimination pathway, rate and extent of gene drugs such as pDNA and antisense oligonucleotides is a prerequisite to designing a good approaches for improving their efficacy. Pharmacokinetic analysis will give us information on the events occurring in the body following drug administration, therefore, it is a powerful tool for developing a strategy to fight the inefficient results of gene therapy trials thus far.

REFERENCES

Agrawal, S., Temsamani, J. and Tang, J.Y. (1991) Pharmacokinetics, biodistribution, and stability of oligodeoxynucleotide phosphorothioates in mice. *Proc. Natl. Acad. Sci. USA*, **88**, 7595–7579.

Agrawal, S., Temsamani, J., Galbraith, W. and Tang, J. (1995) Pharmacokinetics of antisense oligonucleotides. *Clin. Pharmacokinet.*, **28**, 7–16.

Ali, S.A., Eary, J.F., Warren, S.D., Badger, C.C. and Krohn, K.A. (1988) Synthesis and radioiodination of tyramine cellobiose for labeling monoclonal antibodies. *Nucl. Med. Biol.*, **15**, 557–561.

Budker, V., Budker, T., Zhang, G., Subbotin, V., Loomis, A. and Wolff, J.A. (2000) Hypothesis: naked plasmid DNA is taken up by cells *in vivo* by a receptor-mediated process. *J. Gene Med.*, **2**, 76–88.

Butler, T.P., Grantham, F.H. and Gullino, P.M. (1975) Bulk transfer of fluid in the interstitial compartment of mammary tumours. *Cancer Res.*, **35**, 3084–3088.

Deshpande, S.V., Subramanian, R., McCall, M.J., DeNardo, S.J., DeNardo, G.L. and Meares, C.F. (1990) Metabolism of indium chelates attached to monoclonal antibody: minimal transchelation of indium from benzyl-EDTA chelate *in vivo*. *J. Nucl. Med.*, **31**, 218–224.

Dow, S.W., Elmslie, R.E., Willson, A.P., Roche, L., Gorman, C. and Potter, T.A. (1998) *In vivo* tumor transfection with superantigen plus cytokine genes induces tumor regression and prolongs survival in dogs with malignant melanoma. *J. Clin. Invest.*, **101**, 2406–2414.

Fox, S.B., Gatter, K.C., Bicknell, R., Going, J.J., Stanton, P., Cooke, T.G. and Harris, A.L. (1993) Relationship of endothelial cell proliferation to tumor vascularity in human breast cancer. *Cancer Res.*, **53**, 4161–4163.

Fujita, T., Takakura, Y., Sezaki, H. and Hashida, M. (1995) Control of disposition characteristics of proteins by direct cationization in mice. *Pharm. Sci.*, **1**, 371–375.

Gullino, P.M. and Grantham, F.H. (1961) Studies on the exchanges of fluids between host and tumor. I. A method for growing 'tissue-isolated' tumors in laboratory animals. *J. Natl. Cancer Inst.*, **27**, 679–689.

Hunt, C.A., MacGregor, R.D. and Siegel, R.A. (1986) Engineering targeted *in vivo* drug delivery. I. The physiological and physicochemical principles governing opportunities and limitations. *Pharm. Res.*, **3**, 333–344.

Imoto, H., Sakamura, Y., Ohkouchi, K., Atsumi, R., Takakura, Y., Sezaki, H. and Hashida, M. (1992) Disposition characteristics of macromolecules in the perfused tissue-isolated tumor preparation. *Cancer Res.*, **52**, 4396–4401.

Kakutani, T., Yamaoka, K., Hashida, M. and Sezaki, H. (1985) A new method for assessment of drug disposition in muscle: application of statistical moment theory to local perfusion systems. *J. Pharmacokin. Biopharm.*, **13**, 609–631.

Kawabata, K., Takakura, Y. and Hashida, M. (1995) The fate of plasmid DNA after intravenous injection in mice: involvement of scavenger receptors in its hepatic uptake. *Pharm. Res.*, **12**, 825–830.

Kircheis, R., Schuller, S., Brunner, S., Ogris, M., Heider, K.H., Zauner, W. and Wagner, E. (1999) Polycation-based DNA complexes for tumor-targeted gene delivery *in vivo*. *J. Gene Med.*, **1**, 111–120.

Kitajima, I., Shinohara, T., Minor, T., Bibbs, L., Bilakovics, J. and Nerenberg, M. (1992) Human T-cell leukemia virus type I tax transformation is associated with increased uptake of oligodeoxynucleotides *in vitro* and *in vivo*. *J. Biol. Chem.*, **267**, 25881–25888.

Kobayashi, N., Kuramoto, T., Yamaoka, K., Hashida, M. and Takakura, Y. (2001) Hepatic uptake and gene expression mechanisms following intravenous administration of plasmid DNA by conventional and hydrodynamics-based procedures. *J. Pharmacol. Exp. Ther.*, **297**, 1–8.

Leunig, M., Yuan, F., Menger, M.D., Boucher, Y., Goetz, A.E., Messmer, K. and Jain, R.K. (1992) Angiogenesis, microvascular architecture, microhemodynamics, and interstitial fluid pressure during early growth of human adenocarcinoma LS174T in SCID mice. *Cancer Res.*, **52**, 6553–6560.

Li, S., Tan, Y., Viroonchatapan, E., Pitt, B.R. and Huang, L. (2000) Targeted gene delivery to pulmonary endothelium by anti-PECAM antibody. *Am. J. Physiol.*, **278**, L504–L511.

Liu, Y., Mounkes, L.C., Liggitt, H.D., Brown, C.S., Solodin, I., Heath, T.D. and Debs, R.J. (1997) Factors influencing the efficiency of cationic liposome-mediated intravenous gene delivery. *Nat. Biotech.*, **15**, 167–173.

Liu, F., Song, Y.K. and Liu, D. (1999) Hydrodynamics-based transfection in animals by systemic administration of plasmid DNA. *Gene Ther.*, **6**, 1258–1266.

Mahato, R.I., Kawabata, K., Takakura, Y. and Hashida, M. (1995a) *In vivo* disposition characteristics of plasmid DNA complexed with cationic liposomes. *J. Drug Target.*, **3**, 149–157.

Mahato, R.I., Kawabata, K., Nomura, T., Takakura, Y. and Hashida, M. (1995b) Physicochemical and pharmacokinetic characteristics of plasmid DNA/cationic liposome complexes. *J. Pharm. Sci.*, **84**, 1267–1271.

Mahato, R.I., Takemura, S., Akamatsu, K., Nishikawa, M., Takakura, Y. and Hashida, M. (1997) Physicochemical and disposition characteristics of antisense oligonucleotides complexed with glycosylated poly(L-lysine). *Biochem. Pharmacol.*, **53**, 887–895.

Mahato, R.I., Anwer, K., Tagliaferri, F., Meaney, C., Leonard, P., Wadhwa, M.S., Logan, M., French, M. and Rolland, A. (1998) Biodistribution and gene expression of lipid/plasmid complexes after systemic administration. *Hum. Gene Ther.*, **9**, 2083–2099.

Mihara, K., Mori, M., Hojo, T., Takakura, Y., Sezaki, H., Hashida, M. (1993a) Disposition characteristics of model macromolecules in the perfused rat kidney. *Biol. Pharm. Bull.*, **16**, 158–162.

Mihara, K., Hojo, T., Fujikawa, M., Takakura, Y., Sezaki, H. and Hashida, M. (1993b) Disposition characteristics of protein drugs in the perfused rat kidney. *Pharm. Res.*, **10**, 823–827.

Mihara, K., Sawai, K., Takakura, Y. and Hashida, M. (1994) Manipulation of renal disposition of human recombinant superoxide dismutase by chemical modification. *Biol. Pharm. Bull.*, **17**, 296–301.

Miyao, T., Takakura, Y., Akiyama, T., Yoneda, F., Sezaki, H. and Hashida, M. (1995) Stability and pharmacokinetic characteristics of oligonucleotides modified at terminal linkages in mice. *Antisense Res. Develop.*, **5**, 115–121.

Nakajima, S., Koshino, Y., Nomura, T., Yamashita, F., Agrawal, S., Takakura, Y. and Hashida, M. (2000) Intratumoral pharmacokinetics of oligonucleotides in a tissue-isolated tumor perfusion system. *Antisense Nucleic Acid Drug Develop.*, **10**, 105–110.

Nemunaitis, J., Fong, T., Burrows, F., Bruce, J., Peters, G., Ognoskie, N., Meyer, W., Wynne, D., Kerr, R., Pippen, J., Oldham, F. and Ando, D. (1999) Phase I trial of interferon gamma retroviral vector administered intratumorally with multiple courses in patients with metastatic melanoma. *Hum. Gene Ther.*, **10**, 1289–1298.

Nishida, K., Tonegawa, C., Kakutani, T., Hashida, M. and Sezaki, H. (1989) Statistical moment analysis of hepatobiliary transport of phenol red in the perfused rat liver. *Pharm. Res.*, **6**, 140–146.

Nishida, K., Tonegawa, C., Nakane, S., Takakura, Y., Hashida, M. and Sezaki, H. (1990) Effect of electric charge on the hepatic uptake of macromolecules in the rat liver. *Int. J. Pharm.*, **65**, 7–17.

Nishida, K., Eguchi, Y., Takino, T., Takakura, Y., Hashida, M. and Sezaki, H. (1991a) Hepatic disposition characteristics of 111In-labeled lactosaminated bovine serum albumin in rats. *Pharm. Res.*, **8**, 1253–1257.

Nishida, K., Mihara, K., Takino, T., Nakane, S., Takakura, Y., Hashida, M. and Sezaki, H. (1991b) Hepatic disposition characteristics of electrically charged macromolecules in rat *in vivo* and in the perfused liver. *Pharm. Res.*, **8**, 437–444.

Nishida, K., Takino, T., Eguchi, Y., Yamashita, F., Hashida, M. and Sezaki, H. (1992) Pharmacokinetic analysis of uptake process of lactosaminated albumin in rat liver constant infusion experiments. *Int. J. Pharm.*, **80**, 101–108.

Nishikawa, M., Ohtsubo, Y., Ohno, J., Fujita, T., Koyama, Y., Yamashita, F., Hashida, M. and Sezaki, H. (1992) Pharmacokinetics of receptor-mediated hepatic uptake of glycosylated albumin in mice. *Int. J. Pharm.*, **85**, 75–85.

Nishikawa, M., Miyazaki, C., Yamashita, F., Takakura, Y. and Hashida, M. (1995) Galactosylated proteins are recognized by the liver according to the surface density of galactose moieties. *Am. J. Physiol.*, **268**, G849–G856.

Nishikawa, M., Takakura, Y. and Hashida, M. (1996) Pharmacokinetic evaluation of polymeric carriers. *Adv. Drug Deliv. Rev.*, **21**, 135–155.

Nishikawa, M., Takemura, S., Takakura, Y. and Hashida, M. (1998) Targeted delivery of plasmid DNA to hepatocytes *in vivo:* optimization of the pharmacokinetics of plasmid DNA/galactosylated poly(L-lysine) complexes by controlling their physicochemical properties. *J. Pharmacol. Exp. Ther.*, **287**, 408–415.

Nishikawa, M., Yamauchi, M., Morimoto, K., Ishida, E., Takakura, Y. and Hashida, M. (2000) Hepatocyte-targeted *in vivo* gene expression by intravenous injection of plasmid DNA complexed with synthetic multi-functional gene delivery system. *Gene Ther.*, **7**, 548–555.

Nomura, T., Nakajima, S., Kawabata, K., Yamashita, F., Takakura, Y. and Hashida, M. (1997) Intratumoral pharmacokinetics and *in vivo* gene expression of naked plasmid DNA and its cationic liposome complexes after direct gene transfer. *Cancer Res.*, **57**, 2681–2686.

Nomura, T., Koreeda, N., Yamashita, F., Takakura, Y. and Hashida, M. (1998a) Effect of particle size and charge on the disposition of lipid carriers after intratumoral injection into tissue-isolated tumors. *Pharm. Res.*, **15**, 128–132.

Nomura, T., Saikawa, A., Morita, S., Sakaeda (ne Kakutani), T., Yamashita, F., Honda, K., Takakura, Y. and Hashida, M. (1998b) Pharmacokinetic characteristics and therapeutic effects of mitomycin C-dextran conjugates after intratumoural injection. *J. Control Release*, **52**, 239–252.

Ogawara, K., Nishikawa, M., Takakura, Y. and Hashida, M. (1998) Pharmacokinetic analysis of hepatic uptake of galactosylated bovine serum albumin in a perfused rat liver. *J. Control Release*, **50**, 309–317.

Ogawara, K., Hasegawa, S., Nishikawa, M., Takakura, Y. and Hashida, M. (1999) Pharmacokinetic evaluation of mannosylated bovine serum albumin as a liver cell-specific carrier: quantitative comparison with other hepatotropic ligands. *J. Drug Target.*, **6**, 349–360.

Ohkouchi, K., Imoto, H., Takakura, Y., Hashida, M. and Sezaki, H. (1990) Disposition of anticancer drugs after bolus arterial administration in a tissue-isolated tumor perfusion system. *Cancer Res.*, **50**, 1640–1644.

Opanasopit, P., Shiraishi, K., Nishikawa, M., Yamashita, F., Takakura, Y. and Hashida, M. (2001) *In vivo* recognition of mannosylated proteins by hepatic mannose receptors and mannan-binding protein. *Am. J. Physiol.*, in press.

Peng, B., Andrews, J., Nestorov, I., Brennan, B., Nicklin, P. and Rowland, M. (2001) Tissue distribution and physiologically based pharmacokinetics of antisense phosphorothioate oligonucleotide ISIS 1082 in rat. *Antisense Nucleic Acid Drug Develop.*, **11**, 15–27.

Perales, J.C., Ferkol, T., Beegen, H., Ratnoff, O.D. and Hanson, R.W. (1994) Gene transfer *in vivo*: sustained expression and regulation of genes introduced into the liver by receptor-mediated uptake. *Proc. Natl. Acad. Sci. USA*, **91**, 4086–4090.

Phillips, J.A., Craig, S.J., Bayley, D., Christian, R.A., Geary, R. and Nicklin, P.L. (1997) Pharmacokinetics, metabolism, and elimination of a 20-mer phosphorothioate oligodeoxynucleotide (CGP 69846A) after intravenous and subcutaneous administration. *Biochem. Pharmacol.*, **54**, 657–668.

Plautz, G.E., Yang, Z., Wu, B., Gao, X., Huang, L. and Nabel, G.J. (1993) Immunotherapy of malignancy by *in vivo* gene transfer into tumors. *Proc. Natl. Acad. Sci. USA*, **90**, 4645–4649.

Ratajczak, M.Z., Kant, J.A., Luger, S.M., Hijiya, N., Zhang, J., Zon, A. and Gewirtz, A.M. (1992) *In vivo* treatment of human leukemia in a scid mouse model with c-myb antisense oligonucleotides. *Proc. Natl. Acad. Sci. USA*, **89**, 11823–11827.

Robinson, P.J. and Rapoport, S.I. (1987) Size selectivity of blood-brain barrier permeability at various times after osmotic opening. *Am. J. Physiol.*, **253**, R459–R466.

Roth, J.A. and Cristiano, R.J. (1997) Gene therapy for cancer: what have we done and where are we going? *J. Natl. Cancer Inst.*, **89**, 21–39.

Saikawa, A., Nomura, T., Yamashita, F., Takakura, Y., Sezaki, H. and Hashida, M. (1996) Pharmacokinetic analysis of drug disposition after intratumoral injection in a tissue-isolated tumor perfusion system. *Pharm. Res.*, **13**, 1438–1444.

Sakurai, F., Nishioka, T., Saito, H., Baba, T., Okuda, A., Matsumoto, O., Taga, T., Yamashita, F., Takakura, Y. and Hashida, M. (2001) Interaction between DNA-cationic liposome complexes and erythrocytes in an important factor in systemic gene transfer via the intravenous route in mice: the role of the neutral helper lipid. *Gene Ther.*, **8**, 677–686.

Sands, H., Gorey-Feret, L.J., Cocuzza, A.J., Hobbs, F.W., Chidester, D. and Trainor, G.L. (1994) Biodistribution and metabolism of internally ^{3}H-labeled oligonucleotides. I. Comparison of a phosphodiester and a phosphorothioate. *Mol. Pharmacol.*, **45**, 932–943.

Sawai, K., Miyao, T., Takakura, Y. and Hashida, M. (1995) Renal disposition characteristics of oligonucleotides modified at terminal linkages in the perfused rat kidney. *Antisense Res. Develop.*, **5**, 279–287.

Sawai, K., Mahato, R.I., Oka, Y., Takakura, Y. and Hashida, M. (1996) Disposition of oligonucleotides in isolated perfused rat kidney: involvement of scavenger receptors in their renal uptake. *J. Pharmacol. Exp. Ther.*, **279**, 284–290.

Senior, J.H. (1987) Fate and behavior of liposomes *in vivo*: a review of controlling factors. *Crit. Rev. Ther. Drug Carrier Syst.*, **3**, 123–193.

Shlesinger, P.H., Doebber, T.W., Mandell, B.F., White, R., DeSchryver, C., Rodman, J.S., Miller, M.J. and Stahl, P.D. (1978) Plasma clearance of glycoproteins with terminal mannose and *N*-acetylglucosamine by liver non-parenchymal cells. Study with beta-glucuronidase, *N*-acetyl-beta-*D*-glucosamine, ribonuclease B and agalacto-orosomucoid. *Biochem. J.*, **176**, 103–108.

Sun, W.H., Burkholder, J.K., Sun, J., Culp, J., Turner, J., Lu, X.G., Pugh, T.D., Ershler, W.B. and Yang, N.S. (1995) *In vivo* cytokine gene transfer by gene gun reduces tumor growth in mice. *Proc. Natl. Acad. Sci. USA*, **92**, 2889–2893.

Takagi, A., Yabe, Y., Oka, Y., Sawai, K., Takakura, Y. and Hashida, M. (1997) Renal disposition of recombinant human interleukin-11 in the isolated perfused rat kidney. *Pharm. Res.*, **14**, 86–90.

Takagi, A., Yabe, Y., Yoshida, M., Takakura, Y. and Hashida, M. (1998a) Hepatic disposition characteristics of recombinant human interleukin-11 (rhIL-11) in the perfused rat liver. *Biol. Pharm. Bull.*, **21**, 1364–1366.

Takagi, T., Hashiguchi, M., Mahato, R.I., Tokuda, H., Takakura, Y. and Hashida, M. (1998b) Involvement of specific mechanism in plasmid DNA uptake by mouse peritoneal macrophages. *Biochem. Biophys. Res. Commun.*, **245**, 729–733.

Takakura, Y., Fujita, T., Hashida, M. and Sezaki, H. (1990) Disposition characteristics of macromolecules in tumor-bearing mice. *Pharm. Res.*, **7**, 339–346.

Takakura, Y., Fujita, T., Furitsu, H., Nishikawa, M., Sezaki, H. and Hashida, M. (1994) Pharmacokinetics of succinylated proteins and dextran sulfate in mice: implications for hepatic targeting of protein drugs by direct succinylation via scavenger receptors. *Int. J. Pharm.*, **105**, 19–29.

Takakura, Y. and Hashida, M. (1996) Macromolecular carrier systems for targeted drug delivery: pharmacokinetic considerations on biodistribution. *Pharm. Res.*, **13**, 820–831.

Takakura, Y., Mahato, R.I., Yoshida, M., Kanamaru, T. and Hashida, M. (1996) Uptake characteristics of oligonucleotides in the isolated rat liver perfusion system. *Antisense Nucleic Acid Drug Develop.*, **6**, 177–183.

Takakura, Y., Takagi, T., Hashiguchi, M., Nishikawa, M., Yamashita, F., Doi, T. *et al.* (1999) Characterization of plasmid DNA binding and uptake by peritoneal macrophages from class A scavenger receptor knockout mice. *Pharm. Res.*, **16**, 503–508.

Toloza, E.M., Hunt, K., Swisher, S., McBride, W., Lau, R., Pang, S., Rhoades, K., Drake, T., Belldegrun, A., Glaspy, J. and Economou, J.S. (1996) *In vivo* cancer gene therapy with a recombinant interleukin-2 adenovirus vector. *Cancer Gene Ther.*, **3**, 11–17.

Uhlmann, E. and Peyman, A. (1990) Antisense oligonucleotides. A new therapeutic principle. *Chem. Rev.*, **90**, 543–584.

Wagner, E., Plank, C., Zatloukal, K., Cotten, M. and Birnstiel, M.L. (1992) Influenza virus hemagglutinin HA-2 N-terminal fusogenic peptides augment gene transfer by transferrin-polylysine-DNA complexes: toward a synthetic virus-like gene-transfer vehicle. *Proc. Natl. Acad. Sci. USA*, **89**, 7934–7938.

Warren, B.A. (1970) The ultrastructure of the microcirculation at the advancing edge of Walker 256 carcinoma. *Microvasc. Res.*, **2**, 443–453.

Wei, M.X., Tamiya, T., Hurford, Jr., R.K., Boviatsis, E.J., Tepper, R.I. and Chiocca, E.A. (1995) Enhancement of interleukin-4-mediated tumor regression in athymic mice by *in situ* retroviral gene transfer. *Gene Ther.*, **6**, 437–443.

Wolff, J.A., Malone, R.W., Williams, P., Chong, W., Acsadi, G., Jani, A. and Felgner, P.L. (1990) Direct gene transfer into mouse muscle *in vivo*. *Science*, **247**, 1465–1468.

Wu, G.Y. and Wu, C.H. (1988) Receptor-mediated gene delivery and expression *in vivo*. *J. Biol. Chem.*, **263**, 14621–14624.

Yamaoka, K., Tanigawara, Y., Nakagawa, T. and Uno, T. (1981) A pharmacokinetic analysis program (MULTI) for microcomputer. *J. Pharmaco-Dyn.*, **4**, 879–885.

Yoshida, M., Mahato, R.I., Kawabata, K., Takakura, Y. and Hashida, M. (1996) Disposition characteristics of plasmid DNA in the single-pass rat liver perfusion system. *Pharm. Res.*, **13**, 599–603.

Zhang, G., Budker, V. and Wolff, J.A. (1999) High levels of foreign gene expression in hepatocytes after tail vein injections of naked plasmid DNA. *Hum. Gene Ther.*, **10**, 1735–1737.

Zhu, N., Liggitt, D., Liu, Y. and Debs, R. (1993) Systemic gene expression after intravenous DNA delivery into adult mice. *Science*, **261**, 209–211.

Residualizing Indium-111-Radiolabel for Plasmid DNA and Its Application to Tissue Distribution Study

Makiya Nishikawa,*,† Takayuki Nakano,† Takayuki Okabe,† Nobuko Hamaguchi,† Yasuomi Yamasaki,‡ Yoshinobu Takakura,‡ Fumiyoshi Yamashita,† and Mitsuru Hashida†

Departments of Drug Delivery Research and Biopharmaceutics and Drug Metabolism, Graduate School of Pharmaceutical Sciences, Kyoto University, Kyoto 606-8501, Japan. Received March 6, 2003; Revised Manuscript Received July 18, 2003

To develop a suitable vector and an administration technique for in vivo gene transfer, the tissue distribution of plasmid DNA (pDNA) needs to be understood. In this study, a novel residualizing radiolabel for pDNA was developed. 4-[p-Azidosalicylamido]butylamine (ASBA) was coupled with diethylenetriaminepentaacetic acid (DTPA) anhydride, then the conjugate was reacted with pDNA by photoactivation, followed by labeling with [^{111}In]$InCl_3$ to obtain ^{111}In-pDNA. The overall structure of pDNA was well preserved, and the retention of its transcriptional activity was 40–98%. After intravenous injection of ^{111}In-pDNA into mice, about 50% of the radioactivity was recovered in the liver within 3 min. The level remained stable for at least 2 h, followed by a very slow decrease to 45% at 24 h. This contrasted with the results obtained with ^{32}P-pDNA by nick translation, in which a rapid decrease in hepatic radioactivity was observed. The amount of radioactivity in the lung following the administration of polyethyleneimine/^{111}In-pDNA complexes correlates well with the transgene expression. These results indicate that the novel residualizing radiolabel clearly demonstrates the cells that have taken up pDNA and, therefore, gives us useful information about how to design a better approach for nonviral in vivo gene delivery.

INTRODUCTION

The in vivo gene transfer profile required for effective gene therapy, such as target cell-specificity of gene transfer, efficiency and duration of transgene expression, and number of transfected cells, depends on the target disease. These features are determined not only by the properties of the vector used, but also by the nature of the target cells, the route and method of administration, and the tissue distribution of the vector.

On many occasions using nonviral vectors, plasmid DNA (pDNA) encoding a target gene is used to deliver the gene to the target cell. Transgene expression by using pDNA occurs only in cells that have taken up the DNA following its administration. Therefore, the development of a vector and/or an administration technique that achieves the delivery of pDNA to the target cell in an efficient and specific manner is absolutely essential for successful in vivo gene therapy. Various approaches have been reported to improve the efficiency of in vivo gene transfer, such as complex formation with cationic vectors, electroporation, gene gun, and large-volume injection (*1*). These approaches improve the transgene expression by increasing the amount of pDNA delivered to the target cell.

Optimizing in vivo gene transfer by these approaches requires a detailed understanding of the tissue distribution of pDNA. To this end, several tracing methods have been used such as ^{32}P-label by nick translation (*2*, *3*). However, radioactive metabolites, which are generated before and after the cellular uptake of radiolabeled pDNA, often make it extremely difficult to quantitatively analyze the tissue distribution and pharmacokinetics of pDNA. Therefore, pharmacokinetic analyses of tissue distribution of pDNA complex are only possible for very short periods after in vivo administration (*4*, *5*). For studies involving macromolecules such as antibodies, biologically active proteins, polymers, and their drug conjugates, residualizing radiolabels have been developed to trace their tissue distribution. So far, hydrophilic bifunctional chelate-radioactive metal complexes or radioiodination using sugar-containing spacers has been used as residualizing radiolabels for such compounds (*6*–*10*). In these approaches, relatively large, hydrophilic molecules are incorporated into the structure of the radiolabeled adducts. After catabolism, radioactive metabolites that are hydrophilic with a high molecular weight are hardly able to pass through biological barriers such as the plasma and lysosomal membranes (*11*), promising the retention of radioactivity within the cells that have taken up the radiolabeled compound.

In an attempt to study the tissue distribution of pDNA, Bogdanov et al. (*12*) recently reported a ^{99m}Tc-label for pDNA by which the tissue distribution of pDNA can be monitored noninvasively and continuously. However, the linker for the label was cationic and interacted with pDNA in an electrostatic manner. Such an interaction altered the physicochemical properties of pDNA, as shown by agarose gel electrophoresis, which would alter the tissue distribution characteristics of pDNA. In addition to radiolabels, biotin (*13*) or a fluorescent dye (*14*) has been covalently introduced into pDNA by photoactivation. Neves et al. (*14*) found that fluorescently labeled pDNA retains 40% of its transcriptional activity as unlabeled pDNA. Compared with the nick translation

* To whom correspondence should be addressed. M. Nishikawa: Phone 81-75-753-4616; Fax 81-75-753-4614; E-mail makiya@pharm.kyoto-u.ac.jp.
† Department of Drug Delivery Research.
‡ Department of Biopharmaceutics and Drug Metabolism.

10.1021/bc034032y CCC: $25.00
Published on Web 08/19/2003

Scheme 1. Synthesis of DTPA–ASBA Conjugate

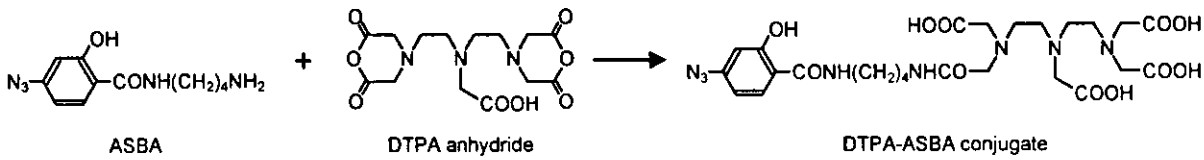

method, the supercoiled structure of pDNA was retained by this technique. In a separate experiment, a peptide nucleic acid clamp was developed as a noncovalent, but highly stable, adduct for pDNA to label it with a fluorescent dye (*15*). These fluorescent labels, however, will be less efficient for tissue distribution studies because they require laborious processing for quantification. The release of metabolites containing the label is another problem as far as the quantitative analysis of the tissue distribution of a labeled pDNA is concerned.

The aim of this study is to develop a residualizing radiolabel for pDNA by which we can quantitatively analyze the tissue distribution of pDNA without needing to consider the efflux of radioactive metabolites from cells. To this end, we have applied a residualizing radiolabel method for pDNA similar to that widely used for radiolabeling proteins: ^{111}In label using a bifunctional chelating agent, diethylenetriaminepentaacetic acid (DTPA). Due to the low degree of reactivity of DTPA anhydride with the primary amino groups in pDNA, we newly designed a chelating agent for pDNA by conjugating DTPA anhydride to 4-[p-azidosalicylamido]butylamine (ASBA) and successfully synthesized DTPA–ASBA conjugate. Then, it was covalently coupled to pDNA by photoreaction followed by ^{111}In radiolabeling. The characteristics of the ^{111}In-pDNA were examined, and then the tissue distribution of radioactivity was investigated in mice after intravenous injection, and compared with data obtained with ^{32}P-labeled pDNA using the nick translation method. Finally, we used ^{111}In-pDNA for analyzing the tissue distribution of pDNA/nonviral vector complex and found the new residualizing radiolabel useful for designing effective gene delivery approaches.

EXPERIMENTAL PROCEDURES

Chemicals. [α-^{32}P]dCTP was obtained from Amersham (Tokyo, Japan). ^{111}Indium chloride ([^{111}In]$InCl_3$) was supplied by Nihon Medi-Physics (Takarazuka, Japan). DTPA anhydride and ASBA were purchased from Dojindo (Kumamoto, Japan) and Pierce, respectively. Fetal bovine serum (FBS) was obtained from Biowhittaker (Walkersville, MD). Opti-MEM I was obtained from Gibco BRL (Grand Island, NY). Dulbecco's modified Eagle's minimum essential medium (DMEM) and other reagents for cell culture were purchased from Nissui Pharmaceutical Co., LTD (Tokyo, Japan). pDNA encoding firefly luciferase cDNA was prepared as previously reported (*16*). Polyethyleneimine (PEI) with an average molecular mass of 10 000 was purchased from Polysciences, Inc. (Warrington, PA). All other chemicals were of the highest grade available.

Radiolabeling of pDNA. To a 27.5 μL of dimethyl sulfoxide solution of ASBA (1 mg) was added DTPA anhydride (2 mg) under dark-room conditions, and the mixture was incubated at room temperature for 1 h to obtain DTPA–ASBA conjugate (Scheme 1). Then, 25 μL of pDNA solution (4 mg/mL) was added to the mixture and the volume was adjusted to 500 μL with phosphate buffered saline (PBS) of pH 7.4. The mixture was immediately irradiated under an UV lamp (365 nm, Ultra-Violet Products, CA) at room temperature for 15 min to obtain DTPA–ASBA coupled pDNA (DTPA–ASBA–pDNA). The product was purified by ethanol precipitation twice, and was dissolved in 20 μL of acetate buffer (0.1 M, pH 6). To 10 μL of sodium acetate solution (1 M) was added 10 μL of [^{111}In]$InCl_3$, then 20 μL of DTPA–ASBA–pDNA. The mixture was incubated at room temperature for 1 h, and unreacted [^{111}In]$InCl_3$ was removed by ultrafiltration. The purity was checked by Sephadex G-25 column (1 × 40 cm) chromatography and 1% agarose gel electrophoresis. The reaction was performed using different amounts of the starting materials, ASBA, DTPA, and pDNA. To determine the number of DTPA bound to pDNA, small amounts of free DTPA were added before radiolabeling with [^{111}In]$InCl_3$, followed by the separation of ^{111}In-pDNA and ^{111}In-DTPA by gel filtration. ^{32}P-labeling of the pDNA was performed as reported previously (*4*).

Animals. All animal procedures were examined by the Ethics Committee for Animal Experiments at the Kyoto University. Female ICR mice (20–25 g) were obtained from the Shizuoka Agricultural Co-operative Association for Laboratory Animals (Shizuoka, Japan).

Transfection to Cultured Cells. HepG2 cells and COS7 cells were obtained from American Type Culture Collection (Manassas, VA) and maintained in DMEM supplemented with 10% FBS at 37 °C under an atmosphere of 5% CO_2 in air. Cells were plated on a 6-well plate at a density of about 2 × 10^5 cells/well (10.5 cm^2) and cultivated in 2 mL of DMEM supplemented with 10% FBS. After 24 h, the culture medium was replaced with medium containing pDNA (2 μg) complexed with 5 μL of Lipofectamine 2000 (Invitrogen). Six hours later, the pDNA complex was removed and the cells were incubated for an additional 18 h. Then, the cells were scraped off and suspended in 200 μL of PBS. The cell suspension was subjected to three cycles of freezing and thawing, followed by centrifugation at 10000*g* for 3 min. Ten microliters of the supernatant was mixed with 100 μL of luciferase assay buffer (Picagene, Toyo Ink, Tokyo, Japan), and the light produced was immediately measured using a luminometer (Lumat LB 9507, EG & G Berthold, Bad Wildbad, Germany). The activity was indicated as the relative light units (RLU) per milligram of cell protein. The protein content of the cell suspension was measured using a protein assay kit (Dojindo, Kumamoto, Japan) and determined with reference to a standard curve for bovine serum albumin.

Transgene Expression in Muscle In Vivo. Control (unmodified) pDNA or DTPA–ASBA–pDNA was injected into the gastrocnemius muscle of anesthetized mice at a dose of 1 μg of pDNA/50 μL of saline. Immediately after injection, electric pulses were applied using a forceps-type electrode. Square-wave electric pulses were generated by a CUY21 electroporator (Nepa Gene, Tokyo, Japan). The parameters of the pulse were fixed at 200 V/cm for the electrical field strength, 20 ms duration, and six pulses. At 2 days after injection, the injected muscle was dissected and subjected to assays for luciferase activity and protein content.

Tissue Distribution of Radiolabeled pDNA after Intravenous Injection. For the tissue distribution

studies, the concentration of ^{32}P- and ^{111}In-pDNA was adjusted by the addition of nonradiolabeled pDNA. Each mouse was injected with ^{111}In-pDNA or ^{32}P-pDNA in saline (10 μg/100 μL). At predetermined periods after injection, groups of three mice each were anesthetized with ether and blood was collected from the vena cava to obtain plasma by centrifugation at 2000g for 2 min. The liver, kidney, spleen, lung, and heart were excised, rinsed with saline, and weighed. ^{111}In-radioactivity of tissue samples was counted in a well-type NaI scintillation counter (ARC-500, Aloka, Tokyo, Japan). ^{32}P-radioactivity was measured in a scintillation counter (LSA-500, Beckman, Tokyo, Japan) after addition of Clear-Sol I (Nacalai tesque, Kyoto, Japan) to tissue sample.

Pharmacokinetic Analysis. Tissue distribution of ^{32}P-pDNA after intravenous injection was pharmacokinetically evaluated based on the clearance concept (*17*). In brief, the change in the amount of a test compound (pDNA) in a tissue with time can be described as follows:

$$\frac{dX_i}{dt} = CL_i C_p - k_{efflux,i} X_i \quad (1)$$

where X_i represents an amount of pDNA in tissue i after administration, C_p is its concentration in plasma, CL_i expresses an apparent tissue uptake clearance from the plasma to tissue i, and $k_{efflux,i}$ represents an efflux rate from tissue i. When the efflux from tissues can be ignored, eq 1 is simplified to

$$\frac{dX_i}{dt} = CL_i C_p \quad (2)$$

Integration of eq 2 from time 0 to t_1 gives

$$CL_i = \frac{X_{i,t_1}}{AUC_{0-t_1}} \quad (3)$$

where AUC is an area under the plasma concentration–time curve of pDNA. According to eq 3, CL_i is obtained by dividing the amount in a tissue by AUC. The total body clearance (CL_{total}) was calculated by fitting an equation to the plasma concentration data of the radioactivity-time profile using the nonlinear least-squares program MULTI (*18*).

Tissue Distribution and Transgene Expression Following Intravenous Injection of PEI/pDNA Complex. pDNA was mixed with PEI at varying ratios and left at room temperature for 30 min. The mixture obtained was subjected to 1% agarose gel electrophoresis to check the complex formation. The N/P ratio, the ratio of the concentration of total nitrogen (N) in PEI to the phosphate groups (P) in pDNA, was used as an index of complex preparation. ^{111}In-pDNA in a free or complexed form with PEI was injected into a mouse tail vein, and the tissue distribution of radioactivity was evaluated 6 h later. In separate experiments, transgene expression in the lung was measured following the injection of naked pDNA or PEI/pDNA complex. In both experiments, the dose of pDNA was fixed at 30 μg/mouse.

RESULTS

Characteristics of ^{111}In-pDNA. Scheme 1 illustrates the chemistry used to prepare DTPA–ASBA conjugate. The product was analyzed by mass spectroscopy, which revealed that DTPA–ASBA was successfully obtained. Then, DTPA–ASBA conjugate was reacted with pDNA, and the final product was labeled with ^{111}In. Table 1 summarizes the reaction conditions and the properties of ^{111}In-pDNA obtained. The number of DTPA–ASBA molecules bound to pDNA was a function of the amounts of ASBA and DTPA in the reaction mixture, and pDNA derivatives with various numbers of DTPA–ASBA molecules could be obtained. The numbers of DTPA–ASBA molecules in pDNA were calculated to be 15.8, 4.1, and 2.3, based on the amounts of radioactivity eluted in pDNA and DTPA fractions (data not shown). The specific activity of ^{111}In-pDNA was as high as about 2×10^6 cpm/μg of pDNA with the largest number of DTPA–ASBA molecules (condition 1).

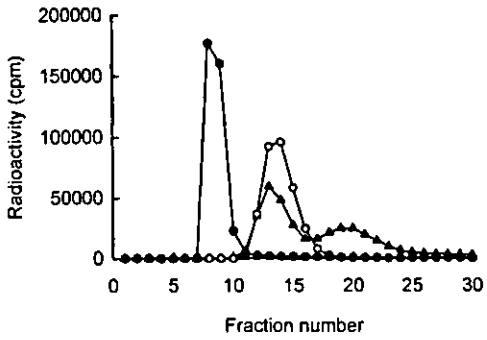

Figure 1. Sephadex G-25 gel filtration profiles of ^{111}In-pDNA, ^{111}In-DTPA, and ^{111}In-DTPA–ASBA. Each sample was applied to a Sephadex G-25 column (1 × 40 cm) and filtrates (40 drops/tube) were collected and radioactivity measured. Keys: (●), ^{111}In-pDNA; (○), ^{111}In-DTPA; (▲), ^{111}In-DTPA-ASBA.

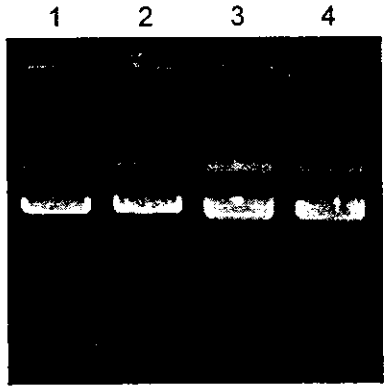

Figure 2. Agarose gel electrophoresis of ^{111}In-pDNA. Ten micrograms of pDNA or ^{111}In-pDNA was applied to 1% agarose gel and run at a constant voltage. pDNA was detected with an UV lamp. For the detection of radioactivity, the gel was cut into pieces and the radioactivity was measured in a γ-counter. Lanes: (1) control pDNA; (2–4) ^{111}In-pDNA (lane 2, condition 3; lane 3, condition 2; lane 4, condition 1).

Table 1. Properties of ^{111}In-pDNA

	reaction conditions				
	pDNA (μg)	ASBA (μg)	DTPA (μg)	no. of DTPA molecules/pDNA	specific activity (cpm/μg of pDNA)
1	100	1000	2000	15.8	2 000 000
2	100	500	1000	4.1	400 000
3	100	250	500	2.3	200 000

^{111}In-pDNA showed only one peak on Sephadex G-25 column chromatography at the void volume, which could be easily distinguished from the peaks of ^{111}In-DTPA and ^{111}In-DTPA–ASBA (Figure 1). On agarose gel electrophoresis, ^{111}In-pDNA showed almost a pattern similar to that of control pDNA (Figure 2). However, the percentages of the open circular and linear forms slightly increased with the increasing number of DTPA–ASBA molecules. The measurement of ^{111}In-radioactivity of the gel indicated that more than 95% of radioactivity were

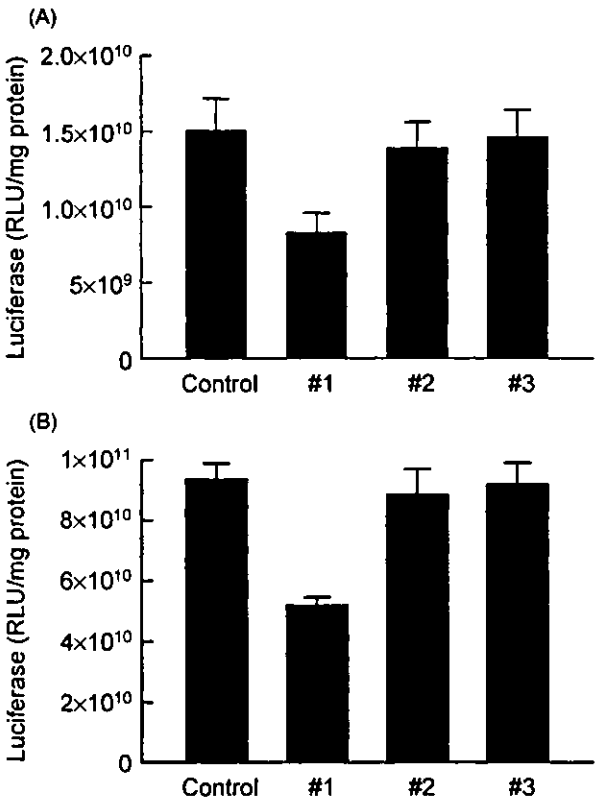

Figure 3. Transgene expression in (A) HepG2 and (B) COS7 cells after transfection of pDNA and DTPA–ASBA–pDNA. Cells (2×10^5 cells) cultured on a 12-well plate were combined with 2 μg of pDNA complexed with Lipofectamine 2000. Results are expressed as the mean ± SD of three wells.

detected at the positions where pDNA was visualized, suggesting that ^{111}In is associated with pDNA. These distribution characteristics of ^{111}In-radioactivity on the gel were confirmed by autoradiography (data not shown).

Transgene Expression. Gene transfection to HepG2 cells and COS7 cells with the control pDNA complex resulted in luciferase activities of 1.5×10^{10} and 9.3×10^{10} RLU/mg of protein, respectively (Figure 3). The transfection activity of the modified pDNA decreased on increasing the number of DTPA–ASBA molecules: about 97–98, 92–94, and 55% of the activity was retained after the modification of 2.3 (condition 3), 4.1 (condition 2), and 15.8 (condition 1) DTPA–ASBA molecules, respectively.

The transfection activity of the pDNA derivatives modified with DTPA–ASBA was also examined in vivo after intramuscular injection followed by electroporation. Again, there was successful transgene expression in mouse muscle with activity 93, 82, and 40% that of the control pDNA, respectively (data not shown). In the following tissue distribution experiments, ^{111}In-pDNA with the highest specific activity (condition 1) was used.

Tissue Distribution and Pharmacokinetic Analysis after Intravenous Injection. Figure 4 shows the plasma concentration (A) and liver accumulation (B) time courses of radioactivity after intravenous injection of ^{111}In- and ^{32}P-pDNA into mice at a dose of 0.5 mg/kg. When ^{111}In-pDNA was injected, radioactivity in plasma rapidly decreased with time, and a large amount of ^{111}In-radioactivity was recovered in the liver (up to 50–60% of the dose), which almost leveled off for 2 h. At 24 h after injection, the radioactivity in the liver remained at about 45% of the injected dose. In a similar fashion, ^{32}P-radioactivity following the injection of ^{32}P-pDNA decreased in plasma with time, and there was

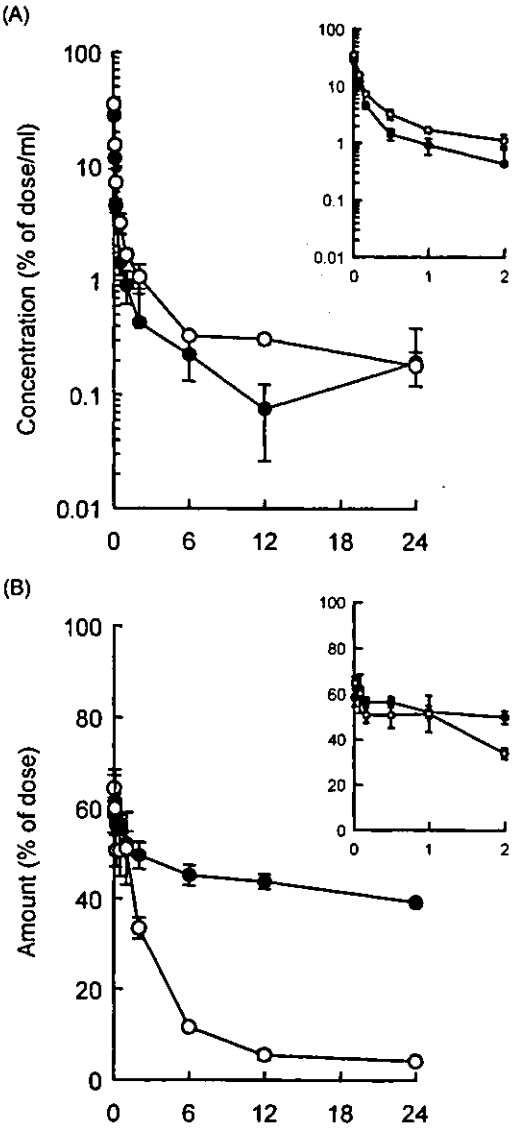

Figure 4. Plasma concentration (A) and liver accumulation (B) time courses of radioactivity in mice after intravenous injection of ^{111}In-pDNA or ^{32}P-pDNA at a dose of 0.5 mg/kg (10 μg/mouse). Keys: (●), ^{111}In-pDNA; (○), ^{32}P-pDNA. Results are expressed as the mean ± SD of three mice.

accumulation in the liver (up to 50–60% of the dose) within 3 min. However, the radioactivity in the liver fell continuously with time down to about 5% of the dose at 12 h. These results obtained with ^{32}P-pDNA were basically similar to previously reported results (*4*, *5*).

The injection of ^{32}P-pDNA resulted in a relatively high, but transient, accumulation of radioactivity in organs such as the kidney, spleen, and lung, whereas ^{111}In-pDNA showed less accumulation of radioactivity in these organs (Figure 5). The urinary excretion of ^{111}In-radioactivity was greater than that of ^{32}P-radioactivity, and about 20% of the injected dose was excreted 30 min postinjection (data not shown).

Table 2 summarizes the AUC and clearances calculated based on the radioactivity at 2 h after intravenous injection of ^{111}In- and ^{32}P-pDNA in mice. ^{111}In-pDNA showed a greater hepatic clearance than ^{32}P-pDNA, reflecting the prolonged retention of radioactivity within the liver. On the other hand, the uptake clearances for the lung, kidney, and heart were greater with ^{32}P-pDNA than with ^{111}In-pDNA.

Distribution and Transgene Expression by PEI/pDNA. Finally, we examined the correlation between the

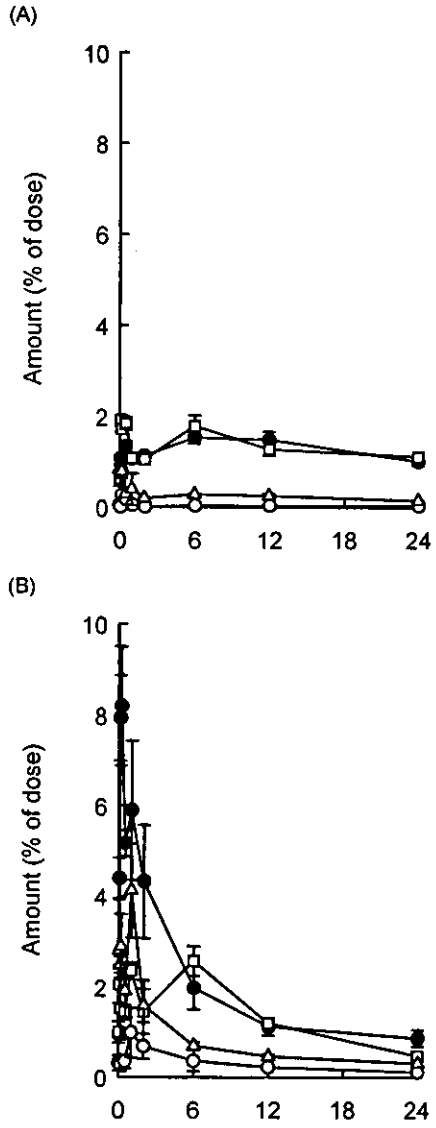

Figure 5. Tissue distribution-time courses of radioactivity in mice after intravenous injection of ^{111}In-pDNA (A) and ^{32}P-pDNA (B) at a dose of 0.5 mg/kg (10 μg/mouse). Keys: (●), kidney; (□), spleen; (△), lung; (○), heart. Results are expressed as the mean ± SD of three mice.

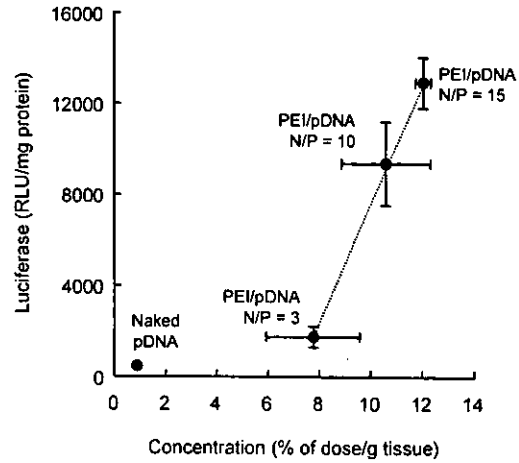

Figure 6. Relation between the concentration of ^{111}In-radioactivity and transgene expression in the lung at 6 h after intravenous injection of (^{111}In-)pDNA at a dose of 30 μg/mouse. Results are expressed as the mean ± SD of three mice.

tissue distribution of ^{111}In-radioactivity and transgene expression in the lung after intravenous injection of PEI/(^{111}In-)pDNA complex into mice. It is well-known that intravenous PEI/pDNA can result in transgene expression in organs with the greatest degree in the lung, and the expression efficiency is at least partially determined by the N/P ratio of the complex (*19*, *20*). In the present experiment, the transgene expression in the lung increased with an increase in the N/P ratio from 0 (naked) to 15. Separately, the delivery of ^{111}In-pDNA to the lung was examined by determining the radioactivity in the lung at 6 h after intravenous injection of PEI/^{111}In-pDNA complex. Then, the expression was plotted against the amount of radioactivity in the organ (Figure 6). As shown in this figure, the expression in the lung correlated well with the amount of ^{111}In-radioactivity in the organ, except for the case of naked ^{111}In-pDNA that showed no significant luciferase activity.

DISCUSSION

Although pDNA amplified in, and extracted from, bacteria is one of the most promising vectors for gene transfer both in vivo and in vitro, its transcriptional activity depends on the functional form of the plasmid: supercoiled (SC), open circular (OC), and linear (L) forms. For example, the OC and L forms of a plasmid were 90 and 10% as efficient as the SC form as far as cell transfection was concerned (*21*). In addition, the chemical and biological properties such as the charge density and the susceptibility to nuclease digestion depend on the structure of pDNA (*22*). Recently, Houk et al. (*23*) reported topoform-dependent pharmacokinetic characteristics of pDNA. Therefore, it is very important to investigate the tissue distribution properties of the pDNA with a structure similar to that used in gene transfer studies, namely, the SC form. To this end, various approaches have been developed to label pDNA with fluorescent probes or radioisotopes under conditions where the SC form of pDNA is hardly altered. These include covalent coupling of a fluorescent dye by photoactivation (*14*), radioiodination of cytidine (*24*), application of a fluorescent peptide nucleic acid clamp (*15*), and metabolic labeling using [^{3}H]thymidine 5′-triphosphate (*25*). Other methods for labeling of pDNA could induce significant changes in the structure. In the present study, although a portion of the chemically modified pDNA showed structural alterations, most of the pDNA retained its SC form. In addition, the modified pDNA retained its transcriptional activity (40−98% as control pDNA), indicating that ^{111}In-pDNA reflects the pharmacokinetic features of the unlabeled pDNA.

Various techniques have been reported to trace externally administered pDNA in vivo. Zelphati et al. (*15*) reported a peptide nucleic acid (PNA)-based fluorescent label for pDNA which was fully transcriptionally active. This approach would be also useful in determining the tissue distribution of pDNA, although one first needs to modify the pDNA of interest to add the PNA binding sites. In addition, the radiolabel makes it much easier to trace the in vivo distribution of labeled pDNA than any fluorescent label. PCR amplification of pDNA with an internal standard can also quantitatively determine the plasma concentration of pDNA after in vivo administration (*26*). An analysis based on agarose gel electrophoresis of samples containing pDNA has been used to monitor the pharmacokinetics of pDNA in rats (*23*). These techniques estimating the amount of pDNA by gel electrophoresis are too laborious, especially when information on the tissue distribution of pDNA is required.

Table 2. AUC and Clearances of Radiolabeled pDNA in Mice

compound	AUC (% of dose h/mL)	clearance (μL/h)					
		total	liver	lung	spleen	kidney	heart
^{111}In-pDNA	2.8	36000	17800	69	374	407	3
^{32}P-pDNA	3.9	25800	8670	408	372	1120	181

^{111}In-labeling has been widely used in tissue distribution studies of proteins, polymers, and particulates. A chelating agent is required for labeling with ^{111}In. DTPA anhydride has long been used as a bifunctional chelating agent for ^{111}In labeling of many different molecules, especially monoclonal antibodies (*27*). Although several studies have demonstrated that other chelating agents such as 1-(4-isothiocyanatobenzyl)ethylenediaminetetraacetic acid (*28*) and a *N*-hydroxysulfosuccinimide ester of 1,4,7,10-tetraazacyclododecane *N,N′,N″,N‴*-tetraacetic acid (*29*) can form more stable chelates with ^{111}In, DTPA-^{111}In chelate has sufficient chelating stability in vivo (*30*). After cellular uptake of ^{111}In-labeled proteins followed by intracellular catabolism, ^{111}In is present as ^{111}In-DTPA-lysine and ^{111}In-DTPA in vivo (*31*). These radioactive metabolites are relatively large in size and highly hydrophilic, both characteristics making them largely unable to cross biological membranes. Therefore, after cellular uptake, the ^{111}In-radioactivity remains within the cells. These characteristics of ^{111}In-labeling are beneficial for evaluating the pharmacokinetic characteristics of various compounds (*17*). This concept has been applied to the radiolabeling of pDNA for the tissue distribution study. The conjugation of DTPA–ASBA to pDNA, which would be governed by the photoreactivity of ASBA to pDNA (*32*), resulted in pDNA derivatives that can be efficiently radiolabeled with ^{111}In. Although the exact structure needs to be elucidated, ^{111}In-radioactivity remained for a significantly long period after systemic administration of ^{111}In-pDNA, indicating that ^{111}In-pDNA has advantages on its tissue distribution studies similar to those of ^{111}In-labeled other macromolecules. As listed in Table 2, ^{111}In-pDNA gave a greater hepatic clearance than ^{32}P-pDNA, although ^{32}P-pDNA was taken up by the liver as fast as ^{111}In-pDNA. Rapid efflux of radioactive metabolites of ^{32}P-pDNA will explain the difference in the hepatic clearance of these two derivatives. The released radioactive metabolites are delivered to other organs such as the lung, kidney, and heart, which increased the clearance values of ^{32}P-pDNA for these organs (Table 2). Tissue uptake clearance is a useful parameter, which can be directly compared with those of others and physiological parameters such as blood flow and the rate of fluid-phase endocytosis (*17*). Therefore, a theoretical design of any delivery approach for pDNA can be achieved by considering the relationships between the characteristics on structures and the pharmacokinetic parameters. The present study clearly indicates that the hepatic clearance of pDNA is 20–25% of the hepatic plasma flow rate, and the clearances for other organs are about 2% or smaller than that for the liver.

As shown in Figure 6, this novel pDNA radiolabeling is very useful for developing better approaches to in vivo gene transfer because the amount of ^{111}In-radioactivity in the lung correlated well with the transgene expression level. These results indicate that the organ level of pDNA delivery is important for the final output. Under the experimental settings used in the present study, about 8% of dose/g of tissue, i.e., 0.8 μg of pDNA/lung, are needed for a detectable expression in this organ. The amount of naked pDNA delivered to the lung was too low for a significant gene expression. In a strict sense, however, the amount of pDNA targeted to the nucleus could be a better index of transgene expression.

In conclusion, a new residualizing radiolabel for pDNA has been successfully developed. The radiolabeled pDNA can nicely designate the tissues and cells that take up the DNA after administration. Because gene transfer only occurs in the cells taking up pDNA, the tissue distribution data of pDNA can be used to evaluate the targeting ability of the vector and administration technique used. Then, a better approach can be developed based on the tissue distribution data of a vector system. Thus, ^{111}In-pDNA is useful not only for evaluating the tissue distribution of pDNA and its complex with a vector system, but also for designing an effective vector for targeted delivery of pDNA.

ACKNOWLEDGMENT

This work was supported in part by a Grant-In-Aid for Scientific Research from the Ministry of Education, Culture, Sports, Science and Technology, Japan, and by a grant from the Ministry of Health, Labour and Welfare, Japan.

LITERATURE CITED

(1) Nishikawa, M., and Huang, L. (2001) Nonviral vectors in the new millennium: delivery barriers in gene transfer. *Hum. Gene Ther. 12*, 861–870.

(2) Rigby, P. W., Dieckmann, M., Rhodes, C., and Berg, P. (1977) Labeling deoxyribonucleic acid to high specific activity in vitro by nick translation with DNA polymerase I. *J. Mol. Biol. 113*, 237–251.

(3) Piatyszek, M. A., Jarmolowski, A., and Augustyniak, J. (1988) Iodo-Gen-mediated radioiodination of nucleic acids. *Anal. Biochem. 172*, 356–359.

(4) Kawabata, K., Takakura, Y., and Hashida, M. (1995) The fate of plasmid DNA after intravenous injection in mice: involvement of scavenger receptors in its hepatic uptake. *Pharm. Res. 12*, 825–830.

(5) Kobayashi, N., Kuramoto, T., Yamaoka, K., Hashida, M., and Takakura, Y. (2001) Hepatic uptake and gene expression mechanisms following intravenous administration of plasmid DNA by conventional and hydrodynamics-based procedures. *J. Pharmacol. Exp. Ther. 297*, 853–860.

(6) Ali, S. A., Eary, J. F., Warren, S. D., Badger, C. C., and Krohn, K. A. (1988) Synthesis and radioiodination of tyramine cellobiose for labeling monoclonal antibodies. *Int. J. Rad. Appl. Instrum. B. 15*, 557–561.

(7) Brandt, K. D., and Johnson, D. K. (1992) Structure–function relationships in indium-111 radioimmunoconjugates. *Bioconjugate Chem. 3*, 118–125.

(8) Demignot, S., Pimm, M. V., Thorpe, S. R., and Baldwin, R. W. (1991) Differences between the catabolism and tumour distribution of intact monoclonal antibody (791T/36) and its Fab/c fragment in mice with tumour xenografts revealed by the use of a residualizing radiolabel (dilactitol-125I-tyramine) and autoradiography. *Cancer Immunol. Immunother. 33*, 359–366.

(9) Deshpande, S. V., Subramanian, R., McCall, M. J., DeNardo, S. J., DeNardo, G. L., and Meares, C. F. (1990) Metabolism of indium chelates attached to monoclonal antibody: minimal transchelation of indium from benzyl-EDTA chelate in vivo. *J. Nucl. Med. 31*, 218–224.

(10) Thorpe, S. R., Baynes, J. W., and Chroneos, Z. C. (1993) The design and application of residualizing labels for studies of protein catabolism. *FASEB J. 7*, 399–405.

(11) Duncan, J. R., and Welch, M. J. (1993) Intracellular metabolism of indium-111-DTPA-labeled receptor targeted proteins. *J. Nucl. Med. 34*, 1728–1738.

(12) Bogdanov, A., Jr., Tung, C. H., Bredow, S., and Weissleder, R. (2001) DNA binding chelates for nonviral gene delivery imaging. *Gene Ther. 8*, 515–522.

(13) Dowty, M. E., Gurevich, V., Berg, R. K., Repetto, G., and Wolff, J. A. (1992) Characterization of biotinylated and gold-labeled plasmid DNA. *Methods Mol. Cell. Biol. 3*, 167–174.

(14) Neves, C., Byk, G., Escriou, V., Bussone, F., Scherman, D., and Wils, P. (2000) Novel method for covalent fluorescent labeling of plasmid DNA that maintains structural integrity of the plasmid. *Bioconjugate Chem. 11*, 51–55.

(15) Zelphati, O., Liang, X., Hobart, P., and Felgner, P. L. (1999) Gene chemistry: functionally and conformationally intact fluorescent plasmid DNA. *Hum. Gene Ther. 10*, 15–24.

(16) Nishikawa, M., Yamauchi, M., Morimoto, K., Ishida, E., Takakura, Y., and Hashida, M. (2000) Hepatocyte-targeted in vivo gene expression by intravenous injection of plasmid DNA complexed with synthetic multi-functional gene delivery system. *Gene Ther. 7*, 548–555.

(17) Nishikawa, M., Takakura, Y., and Hashida, M. (1996) Pharmacokinetic evaluation of polymeric carriers. *Adv. Drug Delivery Rev. 21*, 135–155.

(18) Yamaoka, K., Tanigawara, Y., Nakagawa, T., and Uno, T. (1981) A pharmacokinetic analysis program (multi) for microcomputer. *J. Pharmacobio.-Dyn. 4*, 879–885.

(19) Goula, D., Benoist, C., Mantero, S., Merlo, G., Levi, G., and Demeneix, B. A. (1998) Polyethylenimine-based intravenous delivery of transgenes to mouse lung. *Gene Ther. 5*, 1291–1295.

(20) Morimoto, K., Nishikawa, M., Kawakami, S., Nakano, T., Hattori, Y., Fumoto, S., Yamashita, F., and Hashida, M. (2003) Molecular weight-dependent gene transfection activity of unmodified and galactosylated polyethyleneimine on hepatoma cells and mouse liver. *Mol. Ther. 7*, 254–261.

(21) Adami, R. C., Collard, W. T., Gupta, S. A., Kwok, K. Y., Bonadio, J., and Rice, K. G. (1998) Stability of peptide-condensed plasmid DNA formulations. *J. Pharm. Sci. 87*, 678–683.

(22) Poly, F., Chenu, C., Simonet, P., Rouiller, J., and Monrozier, L. J. (2000) Differences between linear chromosomal and supercoiled plasmid DNA in their mechanisms and extent of adsorption on clay minerals. *Langmuir 16*, 1233–1238.

(23) Houk, B. E., Martin, R., Hochhaus, G., and Hughes, J. A. (2001) Pharmacokinetics of plasmid DNA in the rat. *Pharm. Res. 18*, 67–74.

(24) Terebesi, J., Kwok, K. Y., and Rice, K. G. (1998) Iodinated plasmid DNA as a tool for studying gene delivery. *Anal. Biochem. 263*, 120–123.

(25) Wasan, E. K., Reimer, D. L., and Bally, M. B. (1996) Plasmid DNA is protected against ultrasonic cavitation-induced damage when complexed to cationic liposomes. *J. Pharm. Sci. 85*, 427–433.

(26) Oh, Y. K., Kim, J. P., Yoon, H., Kim, J. M., Yang, J. S., and Kim, C. K. (2001) Prolonged organ retention and safety of plasmid DNA administered in polyethylenimine complexes. *Gene Ther. 8*, 1587–1592.

(27) Hnatowich, D. J., Layne, W. W., Childs, R. L., Lanteigne, D., Davis, M. A., Griffin, T. W., and Doherty, P. W. (1983) Radioactive labeling of antibody: a simple and efficient method. *Science 220*, 613–615.

(28) Meares, C. F., McCall, M. J., Reardan, D. T., Goodwin, D. A., Diamanti, C. I., McTigue, M. (1984) Conjugation of antibodies with bifunctional chelating agents: isothiocyanate and bromoacetamide reagents, methods of analysis, and subsequent addition of metal ions. *Anal. Biochem. 142*, 68–78.

(29) Lewis, M. R., Raubitschek, A., and Shively, J. E. (1994) A facile, water-soluble method for modification of proteins with DOTA. Use of elevated temperature and optimized pH to achieve high specific activity and high chelate stability in radiolabeled immunoconjugates. *Bioconjugate Chem. 5*, 565–76.

(30) Nishikawa, M., Staud, F., Takemura, S., Takakura, Y., and Hashida, M. (1999) Pharmacokinetic evaluation of biodistribution data obtained with radiolabeled proteins in mice. *Biol. Pharm. Bull. 22*, 214–218.

(31) Franano, F. N., Edwards, W. B., Welch, M. J., and Duncan, J. R. (1994) Metabolism of receptor targeted ^{111}In-DTPA-glycoproteins: identification of ^{111}In-DTPA-epsilon-lysine as the primary metabolic and excretory product. *Nucleic Med. Biol. 21*, 1023–1034.

(32) Hermanson, G. T. (1996) Heterobifunctional Cross-linkers. *Bioconjugate Techniques* (Hermanson, G. T., Ed.) pp 228–286, Academic Press, London.

BC034032Y